July 1991 • SERI/TP-214-4394

Structure of Amorphous Silicon and Germanium Alloy Films

Annual Subcontract Report
15 January 1990 - 14 January 1991

R.E. Norberg
P.A. Fedders
Washington University
St Louis, Missouri

olar Energy Research Institute
division of Midwest Research Institute
perated for the U.S. Department of Energy
nder contract No. DE-AC02-83CH10093

July 1991 • SERI/TP-214-4394

Structure of Amorphous Silicon and Germanium Alloy Films

Annual Subcontract Report
15 January 1990 - 14 January 1991

R.E. Norberg
P.A. Fedders
Washington University
St Louis, Missouri

Solar Energy Research Institute
A division of Midwest Research Institute
operated for the U.S. Department of Energy
under contract No. DE-AC02-83CH10093

This publication was reproduced from the best available camera-ready copy submitted by the subcontractor and received no editorial review at SERI.

NOTICE

Printed in the United States of America
Available from:
National Technical Information Service
U.S. Department of Commerce
5285 Port Royal Road
Springfield, VA 22161

Price: Microfiche A01
Printed Copy A03

Codes are used for pricing all publications. The code is determined by the number of pages in the publication. Information pertaining to the pricing codes can be found in the current issue of the following publications which are generally available in most libraries: *Energy Research Abstracts (ERA)*; *Government Reports Announcements* and Index (*GRA* and I); *Scientific and Technical Abstract Reports (STAR)*; and publication NTIS-PR-360 available from NTIS at the above address.

SERI/TP-214-4394 • UC Category: 271 • DE91002191

SERI/TP--214-4394

DE91 002191

Structure of Amorphous Silicon and Germanium Alloy Films

Annual Subcontract Report
15 January 1990 - 14 January 1991

R.E. Norberg
P.A. Fedders
Washington University
St Louis, Missouri

SERI technical monitor: W. Luft

Solar Energy Research Institute
1617 Cole Boulevard
Golden, Colorado 80401-3393
A Division of Midwest Research Institute
Operated for the U.S. Department of Energy
under Contract No. DE-AC02-83CH10093

Prepared under Subcontract No. XB-7-06055-1

July 1991

PREFACE

The main goal of this research has been to improve understanding of the structure of amorphous silicon and germanium alloy films by means of joint theoretical and experimental correlation of results of nuclear magnetic resonance, electron spin resonance, transmission electron microscopy, and other measurements. A major focus of the work is the examination of significant rearrangements of hydrogen which take place under various deposition and post-deposition conditions.

During this fourth year of the project we have applied our CMX 300/200 dual solenoid pulsed Fourier Transform nuclear magnetic resonance (NMR) spectrometer to study hydrogenated and deuterated amorphous silicon and amorphous germanium films. Most of the samples have been prepared by rf glow discharge deposition and characterized[1] by various methods by the group led by William Paul at Harvard University. Other samples have been provided and characterized[2] by Xerox PARC (J. B. Boyce, J. C. Knights, et al.) and Xerox Webster (S. Kaplan, F. Jansen, and M. Machonkin). We also have performed calculations of the effects of strain and coordination on deep electronic states arising from B and P dopants in a-Si and the band tail states in the gap of a-Si arising from strained bonds.

In addition to the collaborations listed above, the work at Washington University relies on participation by three graduate students and on collaborations with faculty colleagues including Professors Anders E. Carlsson, P. C. Gibbons, and K. Kelton. The following members of our research group presently work on the program described here.

Professor Richard E. Norberg	co-principal investigator
Professor Peter A. Fedders	co-principal investigator
Mr. Jeff Bodart	graduate student
Mr. Y. W. Kim	graduate student
Mr. Robert Corey	graduate student

SUMMARY

OBJECTIVES

The primary objective of the research is to improve the understanding at the microscopic level of amorphous silicon and germanium film structures deposited under various methods. The work is to correlate and theoretically analyze NMR, ESR, and other measurements. The alloys of concern include those obtained by adding dopants to hydrogenated silicon and germanium.

The work has been directed to continue deuteron magnetic resonance DMR studies and to pay particular attention to those structural features which may correlate with the photoelectronic properties of the material. The work is to seek an overall correlation of microstructural results with sample preparation conditions and post-deposition history, including anneal-illumination sequences and the light-induced metastability.

DISCUSSION

The provision, by Washington University late in 1987, of a state of the art Chemagnetics CMX 300/200 Dual Solenoid NMR spectrometer has made possible the study of many amorphous silicon and germanium films. DMR spectroscopy of these systems is particularly important because it has been demonstrated[3–5] that DMR can provide detailed structural information on hydrogen (deuterium) in amorphous Si and Ge, including hydrogen rearrangements under various conditions. DMR identifies tightly bound D, weakly bound D, and several species of molecular D_2 and HD. Thus DMR offers the particular opportunity to examine connections between hydrogen arrangements and electrical properties in amorphous silicon and germanium and in their alloys.

The 1990 deuteron magnetic resonance (DMR) accomplishments have included correlation of inhomogeneous nuclear spin relaxation with photovoltaic quality (J. Bodart). The generalized deuteron spin relaxation rate for deuterons tightly bonded to Si or Ge has been shown to correlate monotonically with film photovoltaic quality as characterized by the $\eta\mu\tau$ product. In a second project, a structural rearrangement of atoms has been demonstrated to be associated with the light-induced metastability in a-Si:D,H films (R. Corey). A 150°C dark anneal followed by a room temperature photoillumination produces deuteron magnetic resonance (DMR) spectra which show a difference spectrum composed of two features. There is a quadrupolar doublet, characteristic of a strained bond configuration and a shifted singlet, characteristic of a change in the local magnetic susceptibility. A third approach (Y. Kim) has employed proton-deuteron coupled spin dynamics to examine hydrogen and deuterium motions in high quality films of a-Si:H; a-Si:B,H; a-Si:P,H; and a-Si:D,H. The B- and P-doped films show a significantly enhanced hydrogen mobility above 200 K.

We have also performed a number of detailed calculations on the effects of coordination and strain on the deep electronic states arising from B and P dopants in a-Si as well as the band tail states in the gap of a-Si arising from strained bonds. The calculations show that many dopants can act as either donor or acceptors which should be a factor in explaining the low doping efficiency of a-Si. This work gives a rather complete picture of the effects on the gap states of strains and dopants in the absence of H and for a given configuration of the a-Si network. We have used first principles molecular dynamics simulations to show that the actual equilibrium structure and defect concentration in a-Si is very sensitive to small errors in the description.

We conclude that the methods that we have developed over the past three years are capable of describing many of the effects of strained bonds, especially their effect on dopants. With further work, this could lead to ways of fabricating better samples.

TABLE OF CONTENTS

LIST OF FIGURES

1.0 INTRODUCTION

In published papers[3–5], we have shown that deuteron magnetic resonance (DMR) has the capability to distinguish a variety of deuteron populations in deuterated amorphous silicon, germanium, and their alloys. In the present program we have correlated some of these DMR-determined structural characteristics with electrical transport properties of the films. Hydrogen motional rates are much affected by P and B doping of a-Si:H films. Deuteron spin-lattice relaxation in deuterated a-Ge and a-Si shows an error function type of recovery characteristic of inhomogeneous transport of magnetization. The deduced rate constant decreases monotonically with increasing photoresponse product $\eta\mu\tau$ of the films. It has been found that to a good approximation the rate constant is proportional to the reciprocal of $\sqrt{\eta\mu\tau}$. Proton and deuteron double resonance measurements allow examination of slow atomic rearrangements, manifested in a decay of quadrupolar order. A preliminary cyclic series of dark anneals and photoilluminations of an a-Si:D,H film is accompanied by detectable structural rearrangements. Preliminary examinations of difference spectra show a quadrupolar doublet characteristic of modified deuteron configurations.

2.0 FILM SAMPLES

Deuteron magnetic resonance (DMR) at 30.7 and 46.0 MHz in magnetic fields of 4.7 and 7.0 Tesla has been used to examine a series of film samples of a-Si:D,H; a-Si:D; and a-Ge:D,H prepared[1] at Harvard by the group of W. Paul. These results have been compared with DMR data obtained in samples provided by Xerox PARC (J. B. Boyce, et al.). DMR determines resolved components for tightly bound deuterium (TBD), weakly bound deuterium (WBD), void-contained molecular deuterium (D_2 or DH), rotating silyl groups (SiD_xH_{3-x}), and isolated D_2 and HD trapped in the semiconductor matrix.

For DMR studies the samples were placed in glass or KelF cylinders 2.5 or 5.0 mm o.d. A low Q rf coil was closely wound so that a deuteron $\pi/2$ pulse required 2 μsec. The corresponding 150 Gauss rf field adequately covered the 152 kHz DMR spectral width for deuterons in a-Si:D. Static and flow cryostats provided sample temperatures between 1.6 K and room temperature. Typical DMR signals are weak and often required data averaging over many hours and thousands of scans. To study the light-induced metastability, photoillumination from a tungsten source is conveyed to the film samples within the DMR experimental probe by means of a pair of optical fiber bundles, collimators, and mirrors.

Table 2-1 lists plasma deposition parameters for a series of film samples prepared by W. Paul's group at Harvard. The series consists of pairs of hydrogenated and both hydrogenated and deuterated films of amorphous Si and Ge. All of the Ge films were made at the same rf power, pressure, and gas flows. All of the samples (except 680A and 686A) were deposited on the unpowered electrode. The deposition substrate temperatures were varied as indicated. The deuterated DMR samples were deposited on Al foil which then was removed with dilute HCl or DCl.

Table 2-2 lists deposition parameters for a-Si:D,H and a-Si:H films for which proton and deuteron magnetic resonance measurements have been made of atomic rearrangements as a function of varying temperature and of photoillumination/dark anneal sequences.

Table 2-1 Deposition Parameters for Pairs of Deuterated and Non-Deuterated Films

Sample	T_S (°C)	Power* (watts)	Pressure (Torr)	Flow SiH_4 or GeH_4 (sccm)	Flow H_2 or D_2 (sccm)
H489 Si:H	232	10	0.70	4	76
H541 Si:D,H	230	10	0.70	4	76 D_2
H510 Ge:D,H	261	8	0.95	1	40 D_2
H511 Ge:D,H	260	8	0.95	1	40 D_2
H521 Ge:H	250	8	0.95	1	40
H522 Ge:H	298	8	0.95	1	40
H643 Ge:D,H	301	8	0.95	1	40 D_2
H680 Ge:H	250	8	0.95	1	40
H686 Ge:D,H	250	8	0.95	1	40 D_2
H519 Ge:H	151	8	0.95	1	40
H642 Ge:D,H	151	8	0.95	1	40 D_2
H680A Ge:H	150	8	0.95	1	40
H686A Ge:D,H	150	8	0.95	1	40 D_2

*The average power densities for the depositions were 0.12 W/cm^2 (10 W) and 0.096 W/cm^2 (8 W).

Table 2-2
Deposition parameters of films for which atomic rearrangements have been examined.
(all deposited at a substrate temperature T_s = 230°C)

Film	Type	Power Density ($watts/cm^2$)	Gas Flow
H536	Si:H	0.12	SiD_4 4 sccm H_2 76 sccm
H538	Si:H	0.03	SiH_4 20 sccm
H666	Si:D,H	0.12	SiH_4 4 sccm D_2 76 sccm
XP VI	Si:D,H,B	0.10	SiH_4 9% B_2H_6 1% D_2 90%
XP VII	Si:D,H,P	0.11	SiH_4 9% PH_3 1% D_2 90%

3.0 STRUCTURAL INFERENCES FROM MAGNETIC RESONANCE

3.1 DEUTERON MAGNETIC RESONANCE (DMR) IN AMORPHOUS SILICON AND GERMANIUM

Hydrogen Motions

200 MHz proton NMR has been employed to examine four a-Si:H sample films between 80 and 300K. The purpose has been to measure proton line shapes and relaxation times to look for structural and dynamic differences between samples plasma deposited from SiH_4, $SiH_4 + H_2$, $SiH_4 + B_2H_6 + D_2$, and $SiH_4 + PH_3 + D_2$. Table 2-2 includes some deposition parameters for the films prepared by W. Paul's Harvard group (H) and by Xerox PARC (XP).

All of these high quality samples show the usual proton NMR dual line shape with resolvable broad and narrow components. The presence of H_2 in the starting gas mixture produces proton NMR lines broader by factors of 1 and 1.5 for the broad and narrow lines respectively in H536 than are observed in H538, produced from SiH_4. These line widths indicate the presence of significantly increased hydrogen clustering in H536 produced from $SiH_4 + H_2$.

Proton dynamics also differ among the samples. By 300 K there are motional effects on the dipolar relaxation rate (Γ_{1d}) twice as large in the B and P doped samples XP VI and XP VII than in the undoped samples. These motional effects also become detectable at lower temperatures (<150K) in the B and P doped samples than in the undoped samples (200K). We conclude that there are more rapid hydrogen motions in P and B doped Si than in undoped material. The measurements reveal hydrogen motional characteristic frequencies ranging from 10^3 sec^{-1} to 10^{10} sec^{-1} as the temperature is increased.

Slow and limited hydrogen structural rearrangements have been examined using sensitive DMR methods such as the decay of quadrupolar order in three pulse Jeener-Broeckaert sequences. Figures 3-1 and 3-2 show examples of such measurements at 20 K in a high quality a-Si:D,H film (H541). The rf pulse sequence was $90_x\tau_1 45_y \tau_2 45_y$ with τ_1 = 40 μsec and τ_2 between 2 msec and 10 sec as indicated. In Fig. 3-1 at a repetition interval of 800 sec the quadrupolar order associated with the 66 kHz doublet from tightly bound SiD configurations decays more slowly than does that for the broad central portion of the DMR line. Figure 3-2 shows spectra taken in the presence of HD multiple echoes and at a shorter repetition interval. The HD quadrupolar order measured by the beats in the spectra decays more rapidly with increasing τ_2 than does the broad line underneath the beats, which arises, at least in part, from strained-bond Si:D configurations.

A method has been discovered for manipulating the times of occurrence for the HD multiple DMR echoes in a-Si:D,H. The technique involves proton/deuteron double frequency magnetic resonance and provides the capability to increase the signal strength of selected echoes. This in turn makes possible more rapid measurements of the decay of quadrupolar order which accompanies slow hydrogen rearrangements in the sample films. Figure 3-3 shows the increase in the DMR intensity of the multiple echo (E_4) as the proton pulse

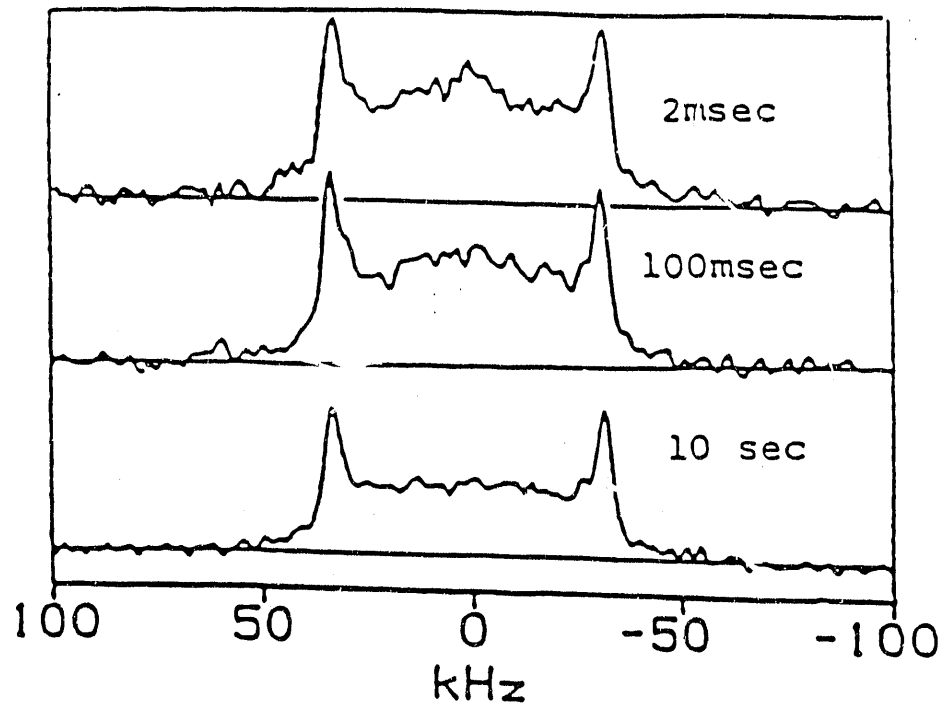

Figure 3-1 Decay of quadrupolar order in central portion of DMR line for a-Si:D,H at 20K and a repetition interval of 800 sec.

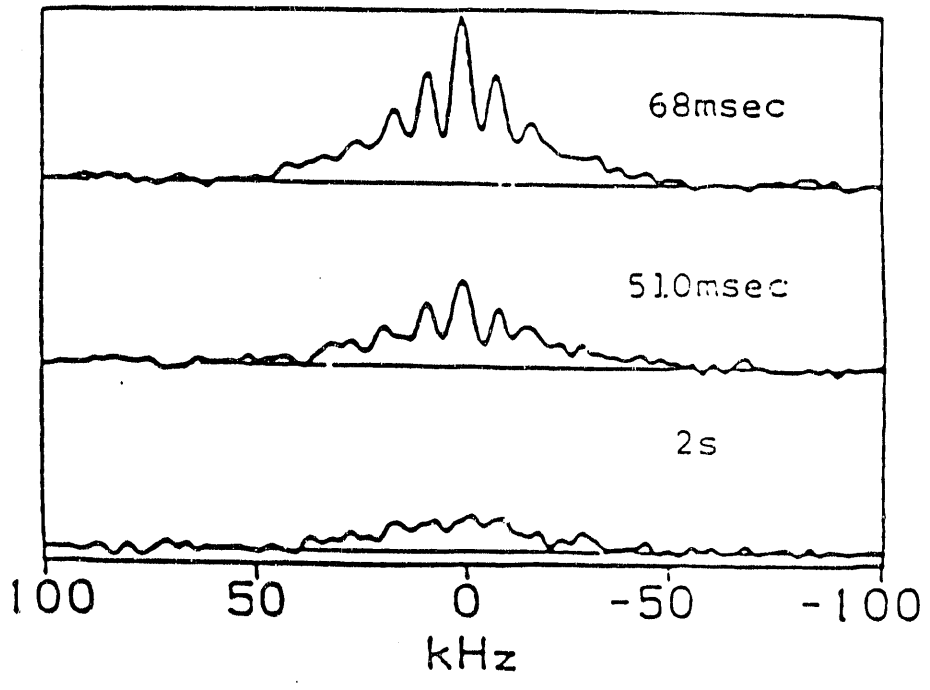

Figure 3-2 Decay of quadrupolar order with τ_1 chosen to reveal beats from HD multiple echoes.

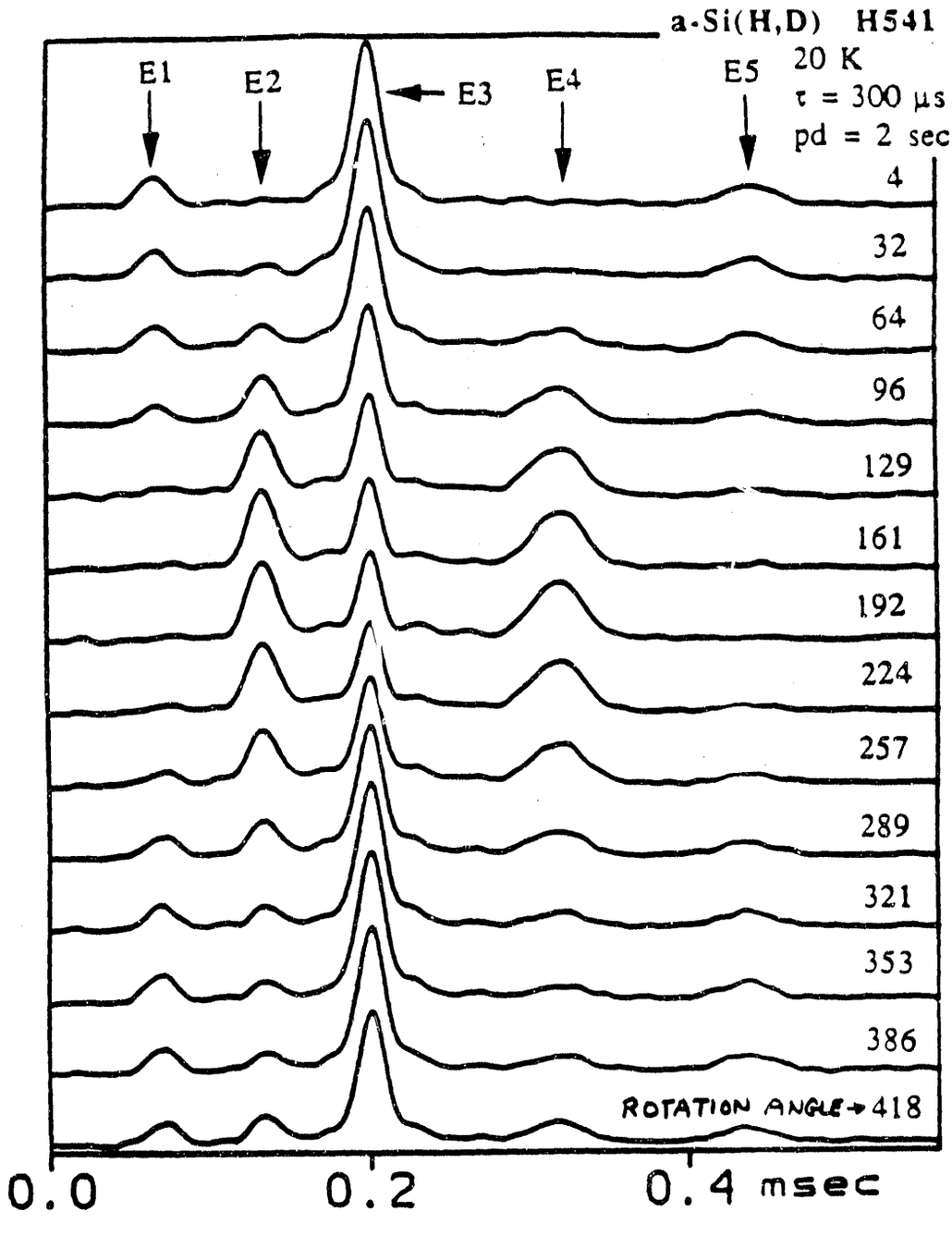

Figure 3-3 Five HD multiple echoes are predicted. As Echoes E1, E3 and E5 decrease, echoes E2 and E4 increase and vice versa. The DMR data are for a-Si:D,H film H541.

rotation angle passes through π. The original echo amplitude is that of E_5 indicated for the 4 degree proton pulse.

We conclude that hydrogen diffusion rates in good plasma-deposited a-Si:H films reach $10^8 sec^{-1}$ at room temperature and $10^9 sec^{-1}$ by 150°C. The activation energy for the hydrogen diffusion is about 0.16 eV/atom. Rates two to three times larger are attained in B-doped films. Deuteron magnetic resonance experiments show that there are faster motional rates at 20 K for molecular HD trapped on nanovoid surfaces than for rearrangements of strained Si-D bonded configurations. Molecular motions show a characteristic rate faster than 1 sec^{-1}, while the strained bonds rearrange at a rate of the order of 0.1 sec^{-1}. Finally, the a-Ge film H686A deposited on the smaller powered electrode not only has the best $\eta\mu\tau$ of the a-Ge series investigated, but it also shows an order of magnitude larger population of hydrogen (and deuterium) than do the samples deposited on the unpowered electrode.

Germanyl Rotors

In past deuteron magnetic resonance (DMR) measurements on deuterated a-Ge films we have not observed the spectral signature of germanyl rotors (GeD_xH_{3-x}). The characteristic 20 kHz inner doublet DMR signal for these rotors has been, if present, obscured by the large narrow central DMR line arising from molecular hydrogen (HD and D_2) in large microvoids in moderate quality a-Ge:D,H. More recent results now show the existence of germanyl rotors.

Figure 3-4 shows DMR spectra at 4.2 K for five deuterated a-Ge:D,H films prepared by W. Paul's group at Harvard. The samples were prepared on the unpowered electrode at various substrate temperatures between 140 and 300°C and at 0.096 W/cm^2, 0.95 Torr, 1 sccm GeH_4, and 40 sccm H_2 or D_2 (cf Table 2-1). The photoresponse functions $\eta\mu\tau$ were determined on similar a-Ge:H films.

In a-Ge sample H642 (Fig. 3-4) where the relative intensity of the DMR narrow central microvoid molecular hydrogen component has decreased to 4%, a 20 kHz germanyl rotor DMR doublet (indicated by arrows) now begins to emerge. The other a-Ge samples may have significant germanyl rotor components masked by their large narrow central lines. It remains to be seen whether or not the germanyl rotor signal can be correlated with the presence of microcrystalline inclusions, as was the case for silyl rotors in a-Si:D,H.

We conclude that germanyl rotors do occur in hydrogenated amorphous germanium films of reasonable quality. Similar populations of silyl rotors do not occur in high quality hydrogenated amorphous silicon, where fewer microvoids occur.

Hydrogen Geometry

A survey has begun of the dynamics of the recoveries of nonequilibrium deuteron magnetization components in a-Si.D,H and a-Ge:D,H. The non-exponential recoveries of deuteron magnetization have been found to be very well described by an error function time dependence. The error function behavior is characteristic of magnetization transport under exceedingly inhomogeneous conditions. Surprisingly even the DMR signal for microvoid-contained HD and D_2 shows a clear error function behavior. Collision with microvoid walls appears to provide an inhomogeneous limitation to the transport. Transport rates and relaxation center concentrations are deduced from the data for a variety of deuterated a-Ge and

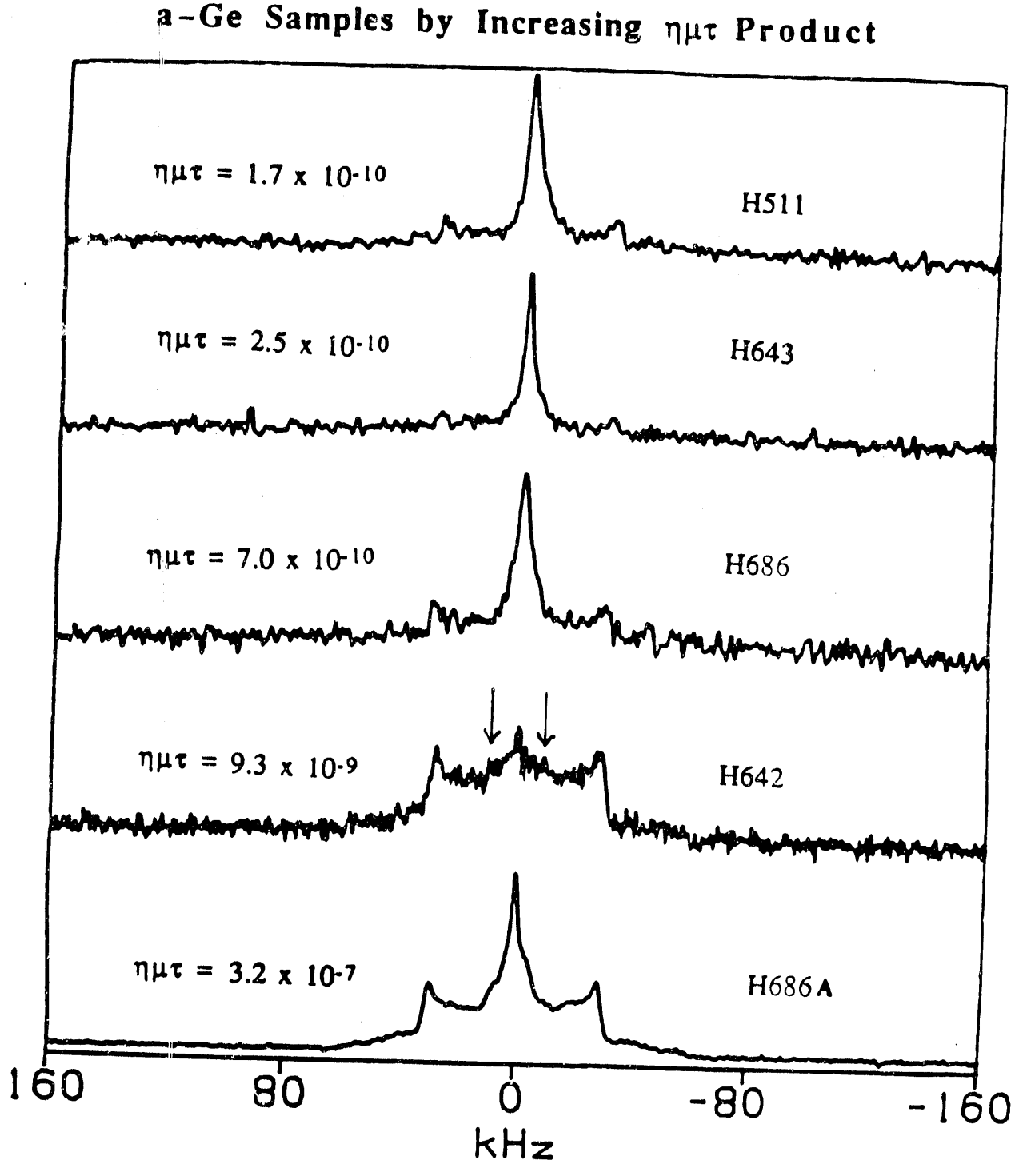

Figure 3-4 DMR lineshapes for five a-Ge:D,H films. H642 shows a germanyl rotor signal, indicated by arrows.

a-Si samples. Information on the local surroundings of the various hydrogen species also are obtained. Samples under investigation include a-Si samples H541 and 666 as well as a-Ge films H642, 643 and 686 (cf. Table 2-1).

The error function transient recovery function turns out to be given by the relations

$$M(t) = [F(c^2\alpha t) - cF(\alpha t)]/(1-c)$$

where

$$F(x) = e^{-x} - (\pi x)^{1/2}\, \mathrm{erf}(x^{1/2})$$

and c is related to the radius of a cluster of nuclear spins that surround a relaxation center.

Figure 3-5 examines the magnetization recovery in a-Ge:D,H (H686A) at 4.2 K. The error function recovery clearly is superior to the exponential fit. Figure 3-6 summarizes transient recovery data for four Ge and one Si sample. Figure 3-7 summarizes the relaxation rate parameters for seven films and correlates them with photoresponse functions $\eta\mu\tau$ determined for similarly-prepared hydrogenated samples (Table 2-1). The straight line through the data corresponds to the relation $1/\alpha = 2.0 \times 10^5 \sqrt{\eta\mu\tau}$ sec.

We conclude that the inverse relaxation rate α^{-1} for tightly bound deuterium (Ge-D and Si-D) nearly is proportional to $\sqrt{\eta\mu\tau}$ over a range of seven orders of magnitude of the photoresponse function $\eta\mu\tau$, from poor a-Ge to excellent a-Ge (and beyond to two high quality a-Si samples which have $\eta\mu\tau$ one to two orders of magnitude larger than the best a-Ge film in the present series). The relaxation rate reflects the proximate populations of paramagnetic dangling bonds and of molecular relaxation centers.

Post-deposition Sample Dynamics - Atomic Rearrangements and the Light-Induced Metastability

We have begun to compare 45 MHz DMR signals for films dark-annealed with those after exposure to light. The experiments are difficult because the anticipated concentration of light induced defects is about 10^{-5}. We have constructed a DMR sample probe designed for *in situ* dark anneal and light soak sequences without otherwise disturbing the film sample. Controlled illumination is conveyed to the sample via dual optical fiber bundles. With this geometry we have observed a reasonable Staebler-Wronski effect as monitored by electron spin resonance (ESR) intensity. Careful measurements are made of DMR difference signals for light soak/dark anneal sequences. We have performed alternating light-soak and dark anneal sequences with intervening DMR studies at 20 and 30 K. The light soaks are for 24 hours at 150 mW/cm^2 using filtered tungsten illumination. The subsequent dark anneals are for 3 hours at 150°C. Our exploratory measurements have proved promising. Figure 3-8 shows DMR difference spectra, recently obtained at 30 K between a light-soaked and 150°C dark annealed high quality a-Si:D,H film sample (H666) (Table 2-2). The repetition interval between rf pulse sequences is short compared to the spin-lattice relaxation time for D tightly-bonded to Si. Thus the difference spectra reflect faster-relaxing weakly-bound D components. The experiments are incomplete and not yet fully analyzed. Nevertheless it is clear that we have reproducible DMR difference spectra associated with post-illumination and post-dark-anneal sequences. We shall examine these difference spectra for various a-Si and a-Ge film samples, for a variety of DMR spectroscopic parameters, and as a function of illumination characterstics. We hope to characterize any detectable hydrogen-silicon

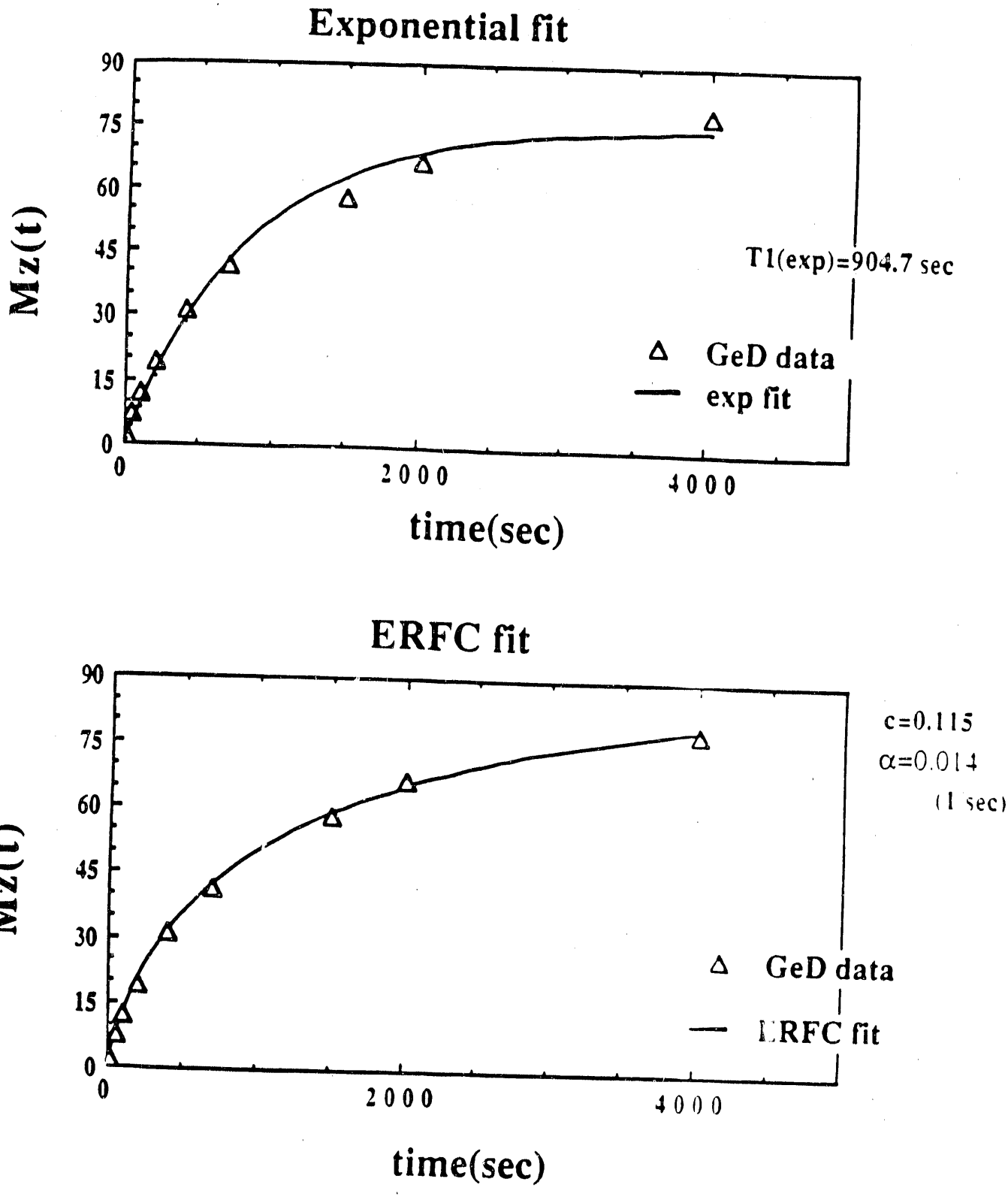

Figure 3-5 Fits to tightly bound deuteron magnetization recovery data in a-Ge:D,H (H686A) at 4.2K. The error function procedure produces a much better fit than does an exponential recovery.

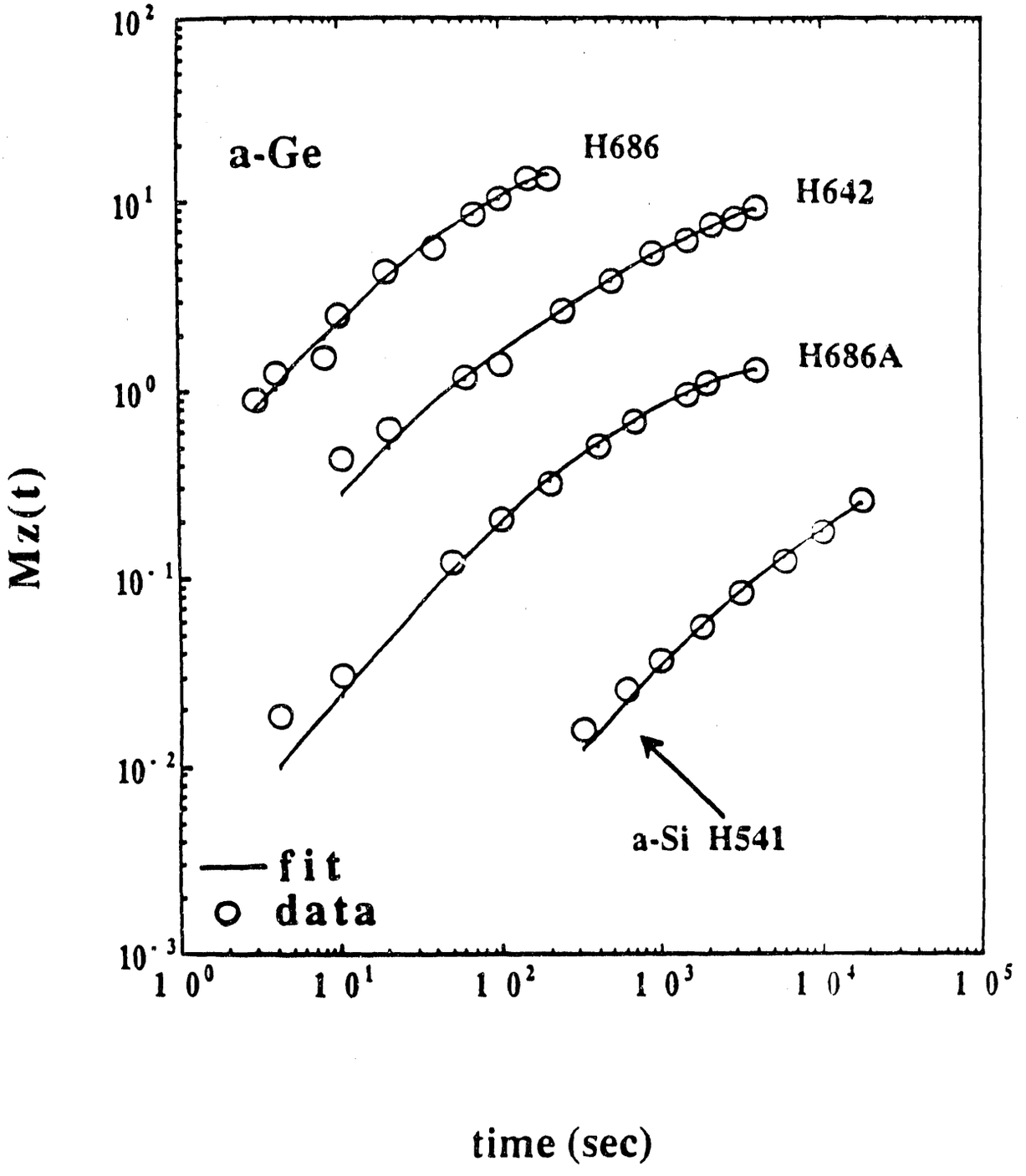

Figure 3-6 Tightly bound deuteron magnetization recoveries for a series of five film samples. The lines indicate error function fits to the transient recoveries.

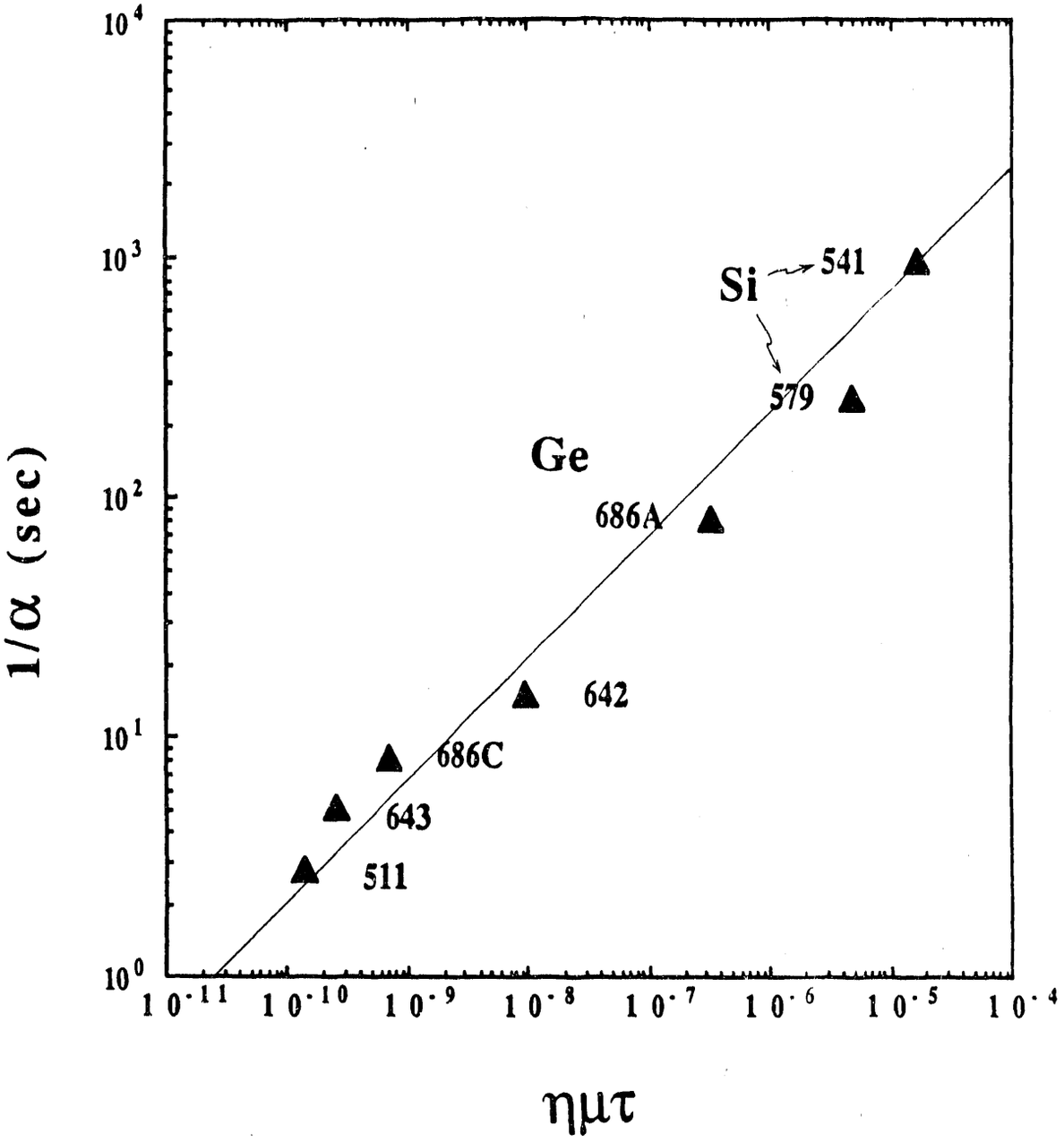

Figure 3-7 The reciprocals of α, the error function relaxation rate parameter for tightly bound deuterium, show a consistent correlation with the photoresponse function ημτ for a series of a-Ge:D,H and a-Si:D,H films. The sloping straight line corresponds to $1/\alpha = 2.0 \times 10^5 \sqrt{\eta\mu\tau}$ sec.

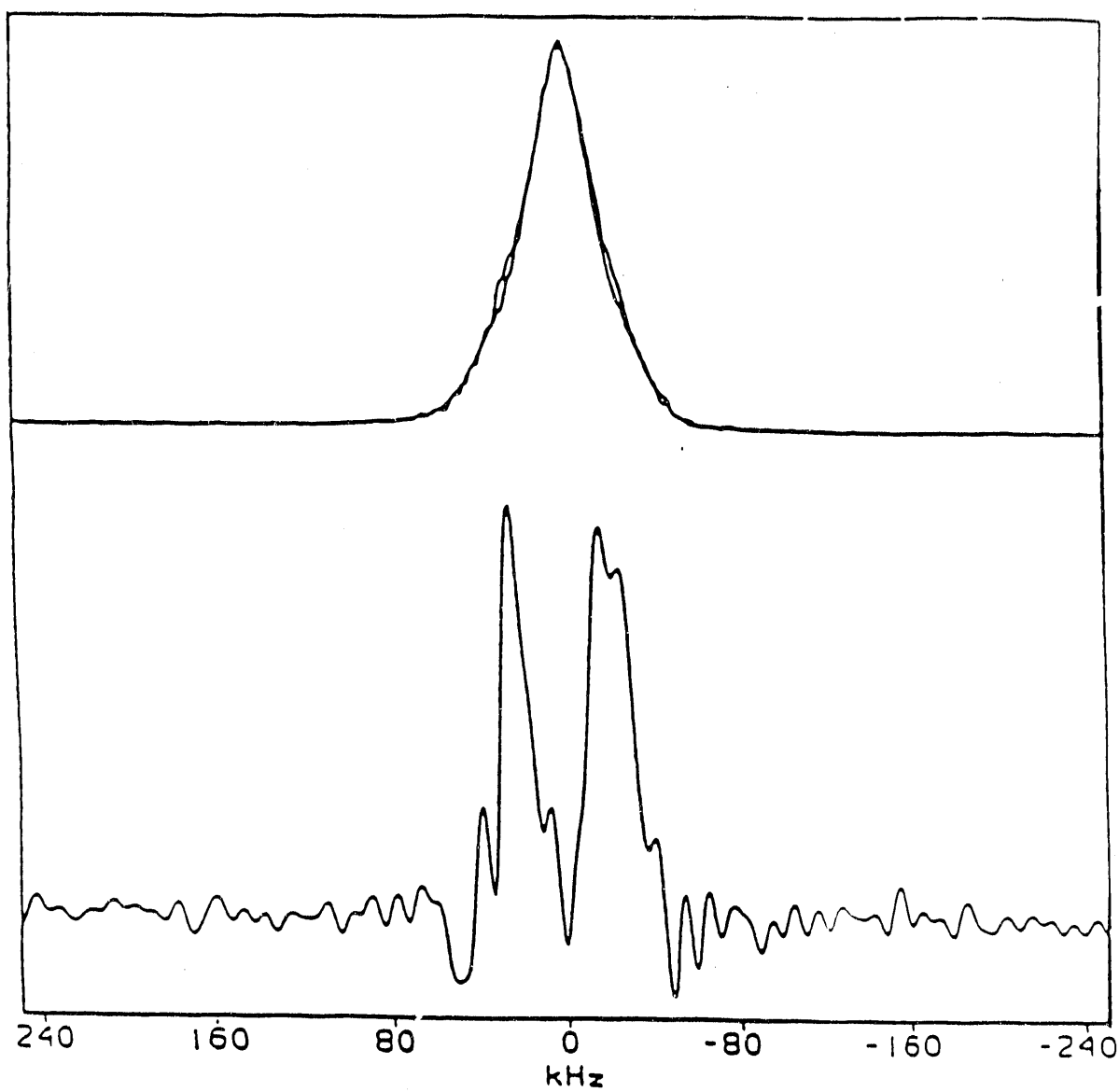

Figure 3-8 (Top) DMR spectra at 30K for light-soaked and 150°C dark-annealed a-Si:D,H (H666).
(Bottom) Difference spectrum light-soaked minus dark-annealed reflects atomic rearrangements which accompany the light-induced metastability.

rearrangements associated with the light-induced metastability. A tentative interpretation of the difference spectrum in Fig. 3-8 is that it reflects an approximately 50 kHz quadrupolar doublet associated with a distinct strained-bond Si-D configuration. There also is a reasonance shift observed in the presence of low temperature illumination. This probably arises from the presence of metastable triplet electron pairs.

Figure 3-9 shows a different DMR comparison sequence in H666 at 30 K. Here the line shapes reflect Fourier transforms of a 2τ echo containing information on fast-relaxing components from both Si-bonded D and molecular HD. The dark-anneal/post-illumination difference spectrum shows both a doublet and a shifted singlet contribution. These difference spectra have repeated in cyclic sequences on H666.

Only speculative and tentative conclusions can be drawn from these preliminary and incomplete experiments. Our present effort is to reduce band pass distortions in the spectra and to examine the difference spectra for various samples, illumination characteristics, and annealing parameters. It is noteworthy that the observed difference spectra reflect changes of order 0.1 to 1% in the presence of a light-induced metastability which involves only ~ 10^{-5} changes in electronic centers. Evidently there is a multipler effect with each light-induced defect related to rearrangements which affect about 100 atoms. We conclude that there are light-induced hydrogen-silicon rearrangements which are detectable with DMR. We hope to achieve structural resolution of these rearrangements in subsequent experiments presently in progress.

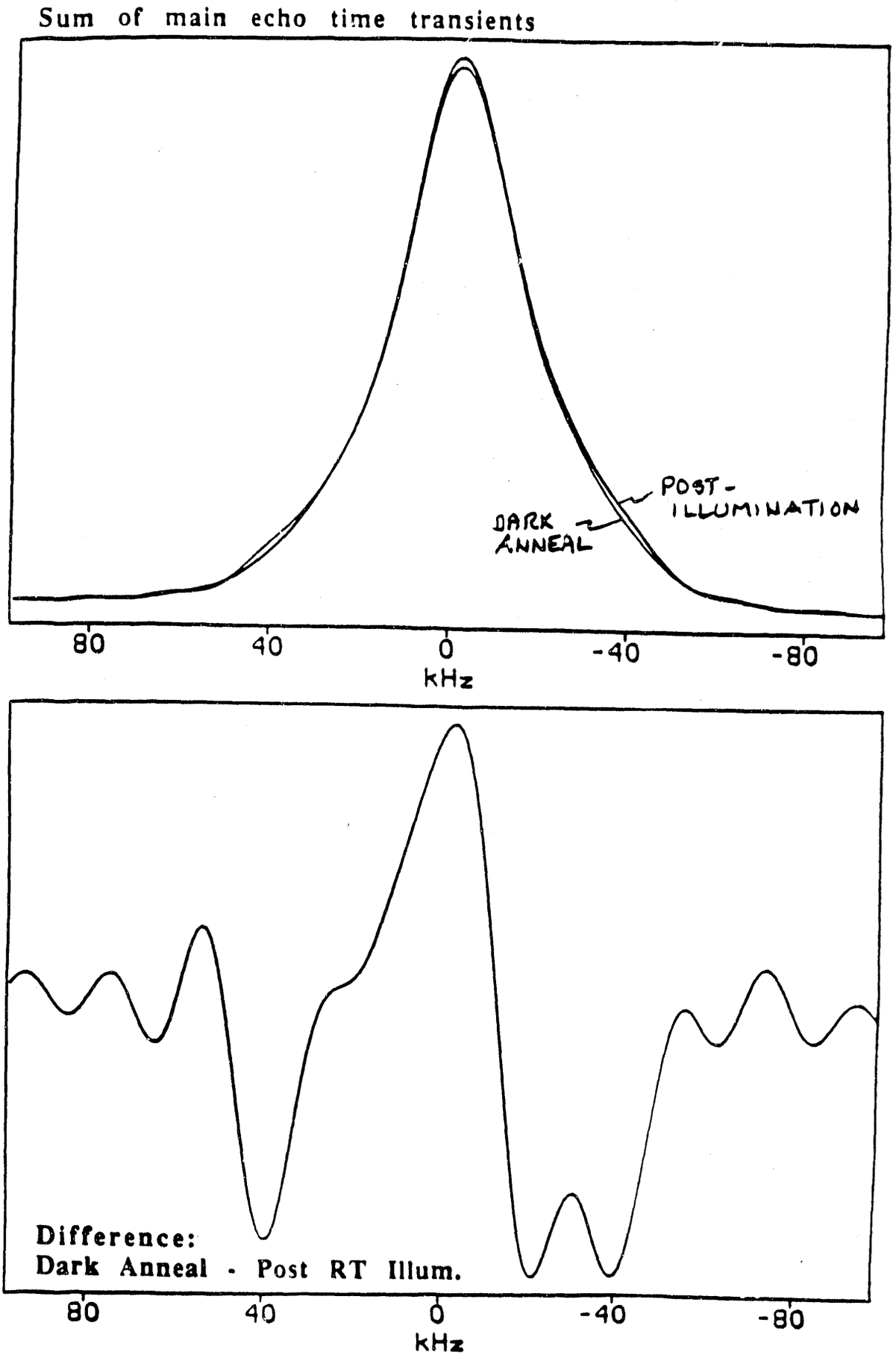

Figure 3-9 DMR spectra and difference spectra for fast-relaxing components of the 2τ echo in a-Si:D,H (H666).

3.2 DEFECTS, TIGHT BINDING, AND FIRST PRINCIPLES MOLECULAR DYNAMICS SIMULATIONS ON a-Si

There have been many theoretical papers on a-Si dealing with electronic structure calculations and molecular dynamics simulations[6–14]. For the electronic structure calculations one always wonders if the sample or cluster that the calculation was performed on was realistic. Furthermore, many calculations on clusters are done using tight binding theory of various forms and degrees of sophistication. We ask the question of how realistic this is or, what properties does it treat reasonably well and what aspects are questionable?

Recent work[15] using first principles molecular dynamics simulations has shown that classical angular dependent forces lead to sizable errors for the forces when the Si samples are not close to crystalline. Further, even smaller errors can lead to large qualitative differences in the actual equilibrium structure and defect concentration. We have made a detailed study of several supercells that were fabricated with Sankey's[16–17] first principles molecular dynamics code. From these supercells we can draw some general conclusions about the nature of the defects found from such simulations and also about the validity of tight binding theory.

We find that tight binding theory gives surprisingly good results for energy eigenvalues and the degree of localization of defect states if some radial dependence is included in the hopping matrix elements. However, for constant matrix element integrals with a cut-off, we obtain poor results. We also find that defect states tend to interact rather strongly with each other even if they are physically separated and that there is not a one-to-one correspondence between geometrical defects and localized states in the gap. This holds whether one uses a tight binding or an *ab initio* band structure. Although there is a tendency to characterize supercells by the number and type of geometrical defects, we find that this is not at all the same as the number and type of localized states in the gap. This appears to be true for supercells with only a few defects or supercells with a larger number of defects.

Here we discuss our 2 defect 63 atom supercell, which is the best supercell that we have fabricated by Sankey's molecular dynamics code. This supercell has been discussed in the literature[7,15] and the coordinates are available upon request. By best we mean the fewest geometrical defects where a geometrical defect is an atom that is not 4-fold coordinated. Although the coordination of an atom depends on the definition of a coordination radius, the number of geometrical defects does not depend critically on this number. Slight variations in the coordination radius often merely shifts defects between 3-fold coordinated (dangling bond) defects and 5-fold coordinated (floating bond) defects. The number density function, $n(r) = 4\pi r^2 \rho g(r)$, for this supercell is given in Fig. 3-10. The first neighbor peak is centered quite close to 2.35Å as expected and there is a reasonably well defined second/third neighbor peak. In fact, the function is reasonably close to pair correlation functions obtained experimentally for good samples[21]. We note that the minimum after the nearest neighbor peak takes place at about 2.85Å and this would form a natural coordination radius for defining a nearest neighbor. Using a number less than this tends to give misleading results. The energy per atom for the supercell is 0.2468 eV/atom with respect to the crystal. This is about a factor of two too big when compared to well annealed material of good electrical quality. However, it is smaller than the energy of any other supercells that we have looked at. The bond angle distribution yields an average bond angle of 109.2° with an rms

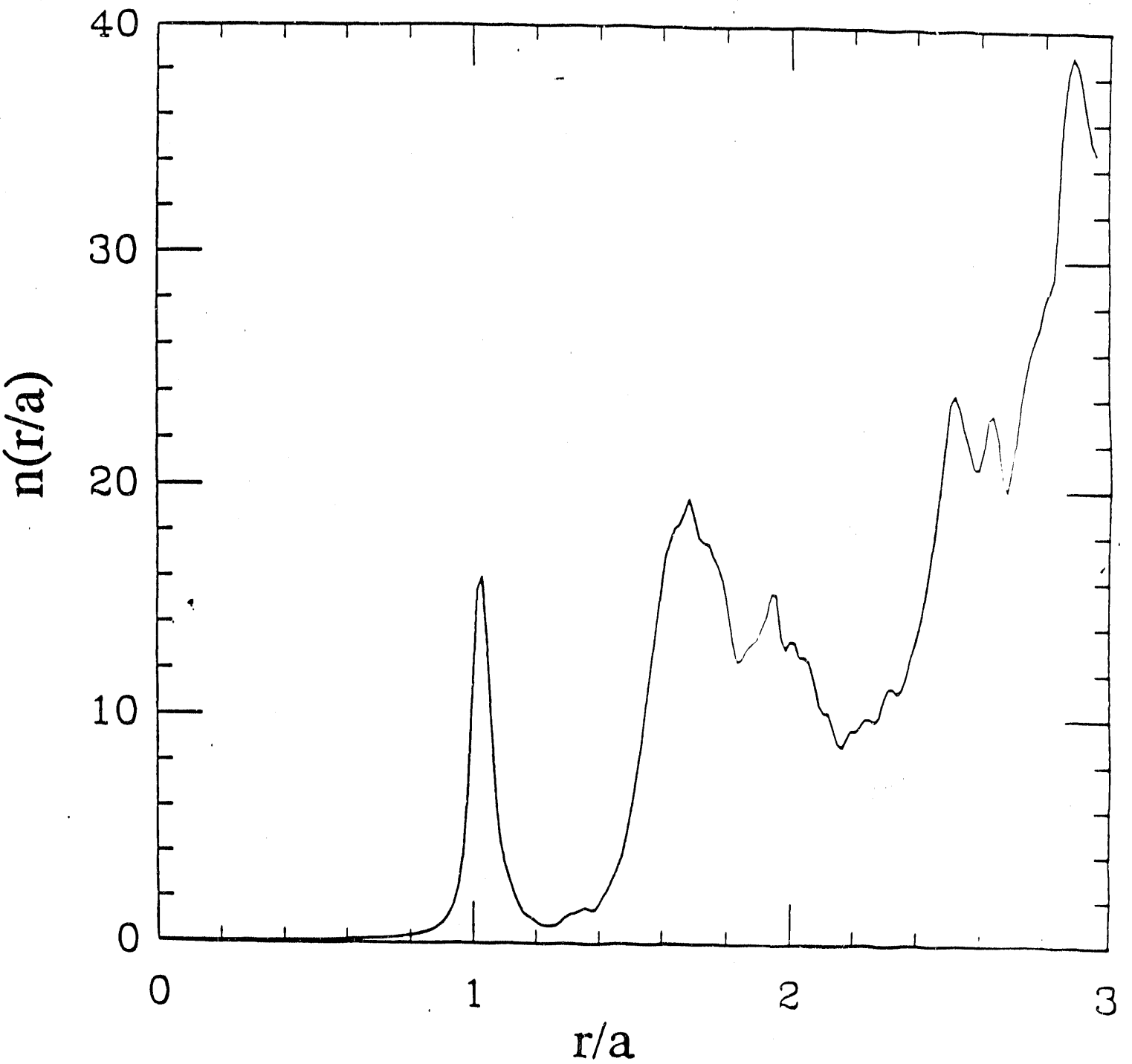

Figure 3-10 Number density function for 2 defect 63 atom supercell.

deviation of 11.0°. These are about what is expected from good computer generated supercells[18].

This supercell exhibits two geometrical defects for any reasonable coordination radius R_o. One of these geometrical defects is a (3-fold coordinated) dangling bond. The other is a dangling bond if $R_o < 2.78$ but is a (5-fold coordinated) floating bond if $R_o > 2.78$. However, both tight binding calculations and local density calculations from the molecular dynamics code show three states in the gap and these three states are the most localized states in the spectrum by quite a margin. There is an important lesson here that geometrical defects are not necessarily the only gap defects (fairly well localized states in the gap). Further, in other supercells, we have always found geometrical defects associated with gap defects but the number of gap defects can be smaller than the number of geometrical defects because more than one geometrical defect can go together to make up a single gap state. Also, gap states can exist that are not correlated with a geometrical defect.

In order to help the reader to visualize the situation we have drawn sketches of the three defect sites (d1,d2, and d3) in Figs. 3-11(a), (b), and (c) respectively. These sketches are merely to indicate the neighbors each atom has as well as some other pertinent data. Unless otherwise noted, interatomic spacings and bond angles are unremarkable and (since the sketches are planar) the bond angles of the sketches are not meaningful. Defect d1, shown in Fig. 3-11(a), is a straight forward 3-fold coordinated dangling bond configuration with its center at atom #56. None of the nearest neighbor or next nearest neighbor atoms to atom #56 are connected with any of the other defects. Thus it would appear to be an isolated defect. Defect d2, shown in Fig. 3-11(b), is what might be called a classic dangling bond/floating bond defect. For a coordination radius $R_o < 2.78$Å the defect is a dangling bond centered at atom #52 while for $R_o > 2.78$Å one would call it a floating bond centered at atom #30. The semantics is, of course, unimportant. Because of the long bond between atoms 30 and 52, previous tight binding Bethe lattice calculations[11,12] would indicate that it acts mostly like a dangling bond as far as energy eigenvalue and localization are concerned. As we shall see, the same conclusion follows from the eigenvalues and localization computed in this paper from either tight binding or local density. The only other noteworthy aspect of Fig. 3-11(b) is that atoms 46 and 51 are nearest neighbors of each other which would not be the case for the more ideal dangling/floating bond defect alluded to above. The last defect, d3, involves only 4-fold coordinated atoms unless one chooses an unreasonably small R_o. The sketch of the defect is given in Fig. 3-11(c) where we have indicated the two interatomic distances that are abnormal and have also designated the bond angles since they are anomalous. Thus the combination of stretched bonds and bond angles that are rather far from tetrahedral combine to form a state in the gap that cannot be characterized as a band tail state. All three defects are reasonably well separated, although the reader should note atom #51 is in both Figs. 3-11(b) and 3-11(c).

Next let us consider the localization of the defect states. Since we are dealing with a supercell of 63 atoms and sp^3 or sp^3s^* bases, the lowest 126 eigenvalues will be occupied and the higher ones will be empty. Eigenvalues 126, 127 and 128 correspond to the most localized states. Table 3-1 summarizes some of the localization analysis for eigenvalue 126. This eigenvalue corresponds to a gap state. We have tabulated localization as defined in a variety of different ways. All of the Q's refer to the fraction of total charge at a site for a given eigenvalue and thus add up to one when summed over all sites. Q(MD) refers to the local

(a)

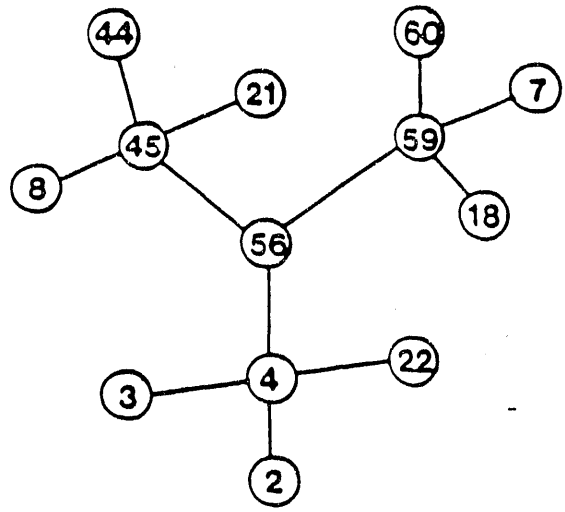

(b)

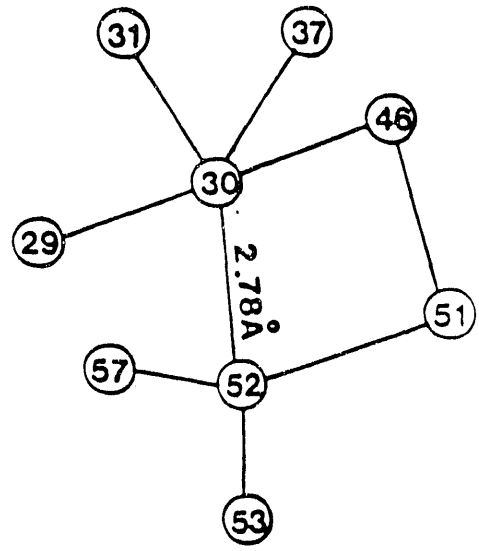

(c)

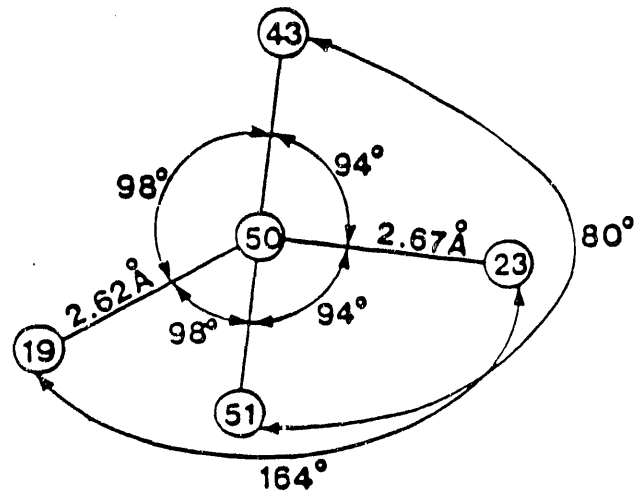

Figure 3-11 Sketches of three defect sites in a-Si.

Table 3-1.

Amount of charge, Q, at various atomic sites for eigenvalue 126 calculated by various methods. The definition of the Q's are given in the text. All atoms with Q > 0.03 by any method are included.

Atom Number	Q(MD)	Q(SW,3.7)	Q(d^{-2},3.2)	Q(const,3.2)	Q(SW,2.7)
4	0.020	0.015	0.004	0.004	0.045
5	0.017	0.032	0.029	0.003	0.002
19	0.032	0.042	0.060	0.026	0.003
22	0.015	0.037	0.040	0.014	0.011
23	0.063	0.155	0.166	0.026	0.008
45	0.015	0.026	0.021	0.010	0.060
56	0.062	0.163	0.138	0.004	0.502
59	0.010	0.013	0.011	0.002	0.047

density value from the molecular dynamics code and, since the orbitals generated by the code extend over several atoms, the atom refers to the center of a small cluster rather than to just one atom. The rest of the Q's are tight binding constructs and refer to just one atom. The tight binding scheme is the sp^3s^* scheme of Vogl *et al.*[20] as modified to Fedders and Carlsson[11] to include distance dependent hopping matrix elements and thereby rendering them useful for a-Si. Thus the Q(MD) and the rest of the Q's should be related but would not be identical even if tight binding were exact. Q(SW,3.7) and Q(SW,2.7) refer to the exponential radial dependence of matrix elements with a Stillinger-Weber[22] type cut-off used in Bethe lattice calculations. The 3.7 and 2.7 refer to the distance in Å where these matric elements are cut-off. $Q(d^{-2},3.2)$ refers to a matrix element that varies as d^{-2} and is cut-off at 3.2Å, while Q(const,3.2) refers to a constant matrix element that is cut-off at 3.2Å. In a perfect crystal, Q would be 1/N for all eigenvalues where N is the number of atoms in the supercell. In these table we have chosen to exhibit all atoms for a given eigenvalue where $Q > 3/N$, or about 0.03, for any of the methods. Consider, for example, Table 3-1 which summarizes the situation for eigenvalue 126. The charge is localized at sites #23 and #56 more than any other sites. As can be seen from Figs. 3-11, site #56 is the site of the dangling bond d1 and site #23 is included in the defect d3. These sites are not particularly close together. Thus we see that the wave functions of different defect states tend to mix even if the defects are not physically right next to each other. The most striking thing about this table is that defect states are far less localized than thos obtained from Bethe lattice calculations with the same tight binding theory as used to calculate Q(SW,3.7). The reason for this was that the defects in the Bethe lattice case were entirely isolated from other defects and also isolated from any strained bonds that were not at the defect site. Thus even a few percent of defects has a major effect on the localization.

The other major lesson to be learned is that tight binding does a pretty good job for the localization of defect states if done with care. In all results we note that Q(const,3.2) and Q(SW,2.7) are very poorly correlated with the "exact" Q(MD). This shows that some radial dependence of the hopping matrix element is necessary in order to obtain a realistic description. Further, too short of a cut-off (2.7Å in this case) also leads to gross inaccuracies. However, with a reasonable radial dependence and a long enough cut-off, decent results are obtained compared to Q(MD). We note the additional advantage of the SW type cut-off that the relevant matrix elements die off smoothly. In studies where the atoms are moving, the eigenvalues do not undergo unphysical discontinuous shifts with time steps. Further, one does not have to arbitrarily define what a nearest neighbor is. One might well ask why the details of the radial dependence are rather unimportant. We believe that the answer is that the radial dependence breaks symmetry in a number of cases and thus a number of unphysical degeneracies or near degeneracies are broken. In particular the correlation between Q(MD) and the tight binding Q's is not very great. Thus while tight binding does reasonably well in describing the localization of the localized states, it appears to have no connection with the actual fluctuations in the wave function at various sites for the extended states. This has interesting implications for the use of tight binding in total energy calculations. That is, while tight binding can yield a respectable electronic density of states, the problems with transferability and sensitivity to computational details make it unreliable for molecular dynamics simulations or total energy calculation involving phase diagrams. For example Paxton[23] and coworkers find structural energy differences much too large compared to accurate calculations of Yin and Cohen[24]. The *ab initio* Sankey code[16] does not have this

problem.

Molecular Dynamics of the Light Induced Defects

We have very recently simulated a proto-Staebler-Wronski effect with our molecular dynamics simulations. There are many theories about how and why light induced defects occur and most of them are quite complicated and involve details of hydrogen and Si dynamics. Our tentative explanation is much simpler and does not involve hydrogen at present. However, our explanation is quantum mechanical in nature and present theories almost totally ignore quantum mechanics.

In our simulations we remove an electron from the highest occupied state which is a defect or dangling bond state. This simulates the ejection of an electron due to light. Because the state from which the electron is removed is quite localized, removal of the electron induced forces on the atoms composing the defect. This induces a general rearrangement of the surrounding atoms, which leads to the formation of more defects. Even when the ejected electron is put back, the system stays in a configuration of more defects because there is a sizable energy barrier prohibiting it from relaxing back to its original state. We note that it is absolutely vital to remove the electron from a localized (defect) state. Removing an electron from an extended state does not change the forces enough to create new defects.

We believe that we can capture the basic physics by performing molecular dynamics simulations on cells as small as 64 (or more recently 216) atoms. That is, the basic mechanism is probably quite local in nature. In fact, our simulations show that the basic mechanism is the changing of the number of electrons on a dangling bond. After this happens, there are relaxation effects which take place over quite large distances.

Our preliminary results indicate that the S-W effect is nucleated by the original dangling bonds. These dangling bonds remain after the illumination and other dangling bonds are formed nearby by not necessarily nearest neighbors the original dangling bond. In a larger supercell, one might find the new dangling bonds even further away.

REFERENCES

1. K. D. Mackenzie, J. R. Eggert, D. J. Leopold, Y. M. Li, S. Lin, and W. Paul, Phys. Rev. B **31**, 2198 (1985).
2. R. A. Street, J. C. Knights, and D. K. Biegelsen, Phys. Rev. B **18**, 1880 (1978).
3. D. J. Leopold, J. B. Boyce, P. A. Fedders, and R. E. Norberg, Phys. Rev. B **26**, 6053 (1982).
4. D. J. Leopold, P. A. Fedders, R. E. Norberg, J. B. Boyce, and J. C. Knights, Phys. Rev. B **31**, 5642 (1985).
5. V. P. Bork, P. A. Fedders, D. J. Leopold, R. E. Norberg, J. B. Boyce, and J. C. Knights, Phys. Rev. B **36**, 9351 (1987).
6. I. Kwon, R. Biswas, G. S. Crest, and C. M. Soukoulis, Phys. Rev. B **41**, 3678 (1990).
7. D. A. Drabold, P. A. Fedders, O. F. Sankey, and J. D. Dow, Phys. Rev. B **42**, 5135 (1990).
8. P. C. Kelires and J. Tersoff, Phys. Rev. Lett. **61**, 562 (1988).
9. R. Biswas, G. S. Grest, and C. M. Soukoulis, Phys. Rev. B **36**, 7437 (1987).
10. W. D. Leudtke and U. Landman, Phys. Rev. B **37**, 4656 (1988).
11. P. A. Fedders and A. E. Carlsson, Phys. Rev. B **37**, 8506 (1988).
12. P. A. Fedders and A. E. Carlsson, Phys. Rev. B **39**, 1134 (1989).
13. R. Car and M. Parrinello, Phys. Rev. Lett. **60**, 204 (1988).
14. I. Stich, R. Car, and M. Parrinello, Phys. Rev. Lett. **63**, 2240 (1989).
15. D. A. Drabold, J. D. Dow, P. A. Fedders, A. E. Carlsson, and O. F. Sankey, Phys. Rev. B **42**, 5345 (1990).
16. O. F. Sankey and D. J. Niklewski, Phys. Rev. B **40**, 3979 (1989).
17. O. F. Sankey, D. J. Niklewski, D. A. Drabold, and J. D. Dow, Phys. Rev. B **41**, 12750 (1990).
18. F. Wooten and D. Weaire, *Solid State Physics*, Vol. 40 (Academic Press), p. 2.
19. M. Schluter and L. J. Sham, *Advances in Quantum Chemistry*, Vol. 21, edited by Samuel B. Tricky (Academic Press), p. 97.
20. P. Vogl, H. P. Hjalmarson, and J. D. Dow, J. Phys. Chem. Solids **44**, 365 (1983).
21. J. Fortner and J. S. Lanin, Phys. Rev. B **39**, 5527 (1989).
22. F. H. Stillinger and T. A. Weber, Phys. Rev. **31**, 5202 (1985).
23. A. T. Paxton, A. D. Satton, and C. M. M. Nex, J. Phys. C **20**, L263 (1987).
24. M. T. Yin and M. L. Cohen, Phys. Rev. B **26**, 5668 (1982).
25. W. Y. Ching, C. C. ;Lin, and L. Guttman, Phys. Rev. B **16**, 5488 (1977).

Document Control Page	1. SERI Report No. SERI/TP-214-4394	2. NTIS Accession No. DE91002191	3. Recipient's Accession No.

4. Title and Subtitle

Structure of Amorphous Silicon and Germanium Alloy Films

5. Publication Date
July 1991

6.

7. Author(s)

R. E. Norberg, P.A. Fedders

8. Performing Organization Rept. No.

9. Performing Organization Name and Address

Department of Physics
Washington University
St. Louis, Missouri

10. Project/Task/Work Unit No.
PV141101

11. Contract (C) or Grant (G) No.

(C) XB-7-06055-1

(G)

12. Sponsoring Organization Name and Address
Solar Energy Research Institute
1617 Cole Blvd.
Golden, CO 80401-3393

13. Type of Report & Period Covered
Technical report,
15 January 1990 - 14 January 1991

14.

15. Supplementary Notes
SERI technical monitor: W. Luft, (303) 231-1452

16. Abstract (Limit: 200 words)

This report describes a research project to improve our understanding of the structure of amorphous silicon and germanium alloy films. This is accomplished by means of theoretical and experimental correlations of the results of nuclear magnetic resonance (NMR), electron spin resonance, transmission electron microscopy, and other measurements. The work focussed on examining the significant rearrangements of hydrogen taking place under various deposition and post-deposition conditions. A CMX 300/200 dual-solenoid pulsed Fourier transform NMR spectroradiometer was used to study hydrogenated and deuterated amorphous silicon and amorphous germanium films. The studies revealed the presence of, and changes in, tightly and weakly bonded hydrogen, molecular hydrogen, and rotating silyl and hydrogen molecules trapped on nanovoid surfaces. Theoretical calculations reveal serious errors in many computer simulations of amorphous solid and liquid silicon.

17. Document Analysis
a. Descriptors
photovoltaics ; solar cells ; amorphous state ; silicon ; germanium ; alloys ; film growth

b. Identifiers/Open-Ended Terms

c. UC Categories
271

18. Availability Statement
National Technical Information Service
U.S. Department of Commerce
5285 Port Royal Road
Springfield, VA 22161

19. No. of Pages
31

20. Price
A03

Form No. 0069E (6-30-87)